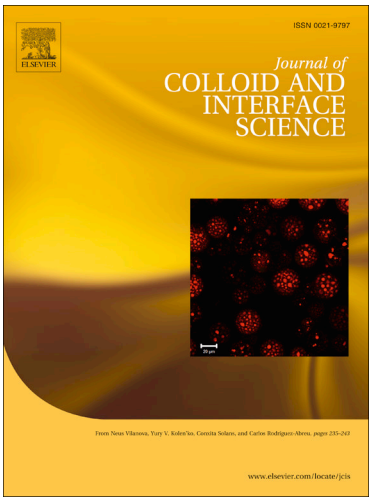

Electrocatalytic activity of manganese oxide nanosphere immobilized onto deoxyribonucleic acid modified electrode: application to determine environmental pollutant thiourea at natural pH

Afshin Maleki, Hiua Daraei, Nader Amini

PII: S0021-9797(17)30672-0
DOI: http://dx.doi.org/10.1016/j.jcis.2017.06.016
Reference: YJCIS 22443

To appear in: *Journal of Colloid and Interface Science*

Received Date: 23 March 2017
Revised Date: 3 June 2017
Accepted Date: 6 June 2017

Please cite this article as: A. Maleki, H. Daraei, N. Amini, Electrocatalytic activity of manganese oxide nanosphere immobilized onto deoxyribonucleic acid modified electrode: application to determine environmental pollutant thiourea at natural pH, *Journal of Colloid and Interface Science* (2017), doi: http://dx.doi.org/10.1016/j.jcis.2017.06.016

Electrocatalytic activity of manganese oxide nanosphere immobilized onto deoxyribonucleic acid modified electrode: application to determine environmental pollutant thiourea at natural pH

Afshin Maleki, Hiua Daraei, Nader Amini*

Environmental Health Research Center, Kurdistan University of Medical Sciences, Sanandaj, Iran

Abstract

Based on immobilizing manganese oxide nanospheres (MnOxNsph)/deoxyribonucleic (DNA) on glassy carbon electrode (MnOxNsph/DNA/GCE), a new electrochemical biosensor for the detection of thiourea (TU) was fabricated. In order to prepare DNA template, cyclic voltammetry (CV) method was used. Scanning electron microscopy (SEM) was used for characterization of MnOx/DNA. Electrochemical impedance spectroscopy was utilized to confirm the successful stepwise assembly procedure of the biosensor. The electrocatalytical behaviors of the biosensor were also investigated by cyclic voltammetry and differential pulse voltammetry (DPV). The results showed that MnOxNsph/DNA exhibited a remarkable electrocatalytic activity for the oxidation of TU under optimal conditions. The linear range, detection of limit and sensitivity were calculated for oxidation peaks (OX1 and OX2). This electrode demonstrated many advantages such as high sensitivity, low detection of limit, excellent catalytic activity at natural pH values, remarkable antifouling property toward TU and its oxidation product for the two oxidation peaks.

Keywords: DNA; Manganese oxide nanosphere; Thiourea; Biosensor; Amperometry

---

*Corresponding author: Email address: naderamini5@yahoo.com, naderamini95@yahoo.com, Tel: +98 9183761209

1. Introduction

Thiourea (TU) has extensively been employed in various fields of science, technology, and industry for different purposes. For example in industry it is used in rubber industry; in agriculture it is used as fungicides and herbicides [1]; in electroplating industry [2], it is used as a substance that improves the ripening of fruit species [3]; in analytical chemistry [4-5], it is used as a photocatalyst [6], and polarization filters[7]; and it is used in electronic industry, including electronic modulators and electro-acoustic devices [8],and photography [9].

Thiourea is known to be an important environmental pollutant with harmful effects on mammalian species [10]. Moreover, it induces hypothyroidism which causes damage to pulmonary endothelial cells and possibly mesothelial lining cells in animal organisms. It is also assumed that thioureas inhibit nitrification in water and soil [11].

Terefore, the development of accurate and reliable methods for determination of thiourea is assumed to be practically important. Many analytical methods have been proposed for the anaysis of TU, among which the followings are well-known: high-performance liquid chromatography (HPLC)[12], flow injections method [13], spectrophotometry [9], mass spectrometry [14], fourier transform infrared spectroscopy (FTIR) [15] and Raman spectroscopy [16] techniques.

However, spectrophotometric method is based on derivatization with cromogenic reagents. In addition, chromatographic separation-based methods present some disadvantages as the derivatization and extraction stage of the procedure can increase analysis time, the total cost of the assay and is also complicated [17]. On the other hand, fast and simple methods with minimal sample pretreatment are needed for the determination of TU. Electrochemical techniques can be proposed as the most favored methods for the determination of sulfur compounds (for example thiourea).The electrochemical analysis of sulfur compounds (such as TU) at the surface of conventional electrodes (e.g., glassy carbon and Boron-Doped Diamond) encounters drawbacks such as a sluggish electrochemical process and it requirement high overpotentials [18-20].

To overcome these problemes, many strategies have been proposed. One of these methods is the modification of the surface of the conventional electrodes with different materials

such as a polymeric layer [21], composite materials [22], metallic complexes [23], nanoparticles [24] and organic compounds [25].

It is obvious that the size and shape of nanostructures play a significant role in their various applications [26]. In general, two different routes are proposed to access these ordered nanomaterials: one is using an appropriate template precursor, and the other one is controlling selected parameters to arrange the components for multidimensional morphologies [27]. Biomaterials assembled on appropriate surfaces can provide templates for the immobilization of nanomaterials or nanopartilcles (NPs) which lead to the construction of new NP-biomolecule hybrid systems [28]. Among different types of biomaterials, deoxyribonucleic acid (DNA) has been used as an inexpensive, controllable and easily adaptable material with physical and chemical properties that can be appropriate to fabricate metalic nanostructures [29-30].

A growing number of researchers have exploited the properties of deoxyribonucleic acid [31-32] to fabricate advanced materials for electrochemical biosensor, energy conversion devices, electronic circuits, medical devices and energy storage [33]. Single-stranded DNA has been used for the construction of single-walled carbon nanotubes (CNTs) by forming p-stacking between the DNA base pair and the carbon ring of nanotubes CNTs [34]. Apart from these, different types of metals, metal oxides or even semi-conductor nanowires like Au[35], Ag[36], Pd[37], Pt[38], Fe2O3[39] and CdS[40], have been immobilized onto DNA templates.

Studies show that among different oxide materials, due to its physical and chemical properties as well as wide applications in electrochemical sensors, ion exchange, catalysis, molecular adsorption and energy storage devices [27], manganese oxide is considered as one of the most attractive inorganic materials,.

In this paper, we have reported a kind of electrochemical method to prepare manganese oxide nanoshere with DNA as a template. We also have shown its application in the electrocatalytic oxidation of TU in 0.1M pH 7 phosphate buffer.

2. Experiment

2.1. Reagents

Double strain DNA (dsDNA) was purchased from Sigma-Aldrich and used as received. Buffer solutions (0.1 M) were prepared from di- sodium hydrogen phosphate (Na_2HPO_4), $MnSO_4.2H_2O$, sodium dihydrogen phosphate (NaH_2PO_4), sodium sulphate (Na_2SO_4), hydrogen chloride (HCl), sodium hydroxide (NaOH), and hydrogen peroxide obtained from Merck.

2.2. Apparatus

Electrochemical experiments were performed with a three-electrode system, consisting of an Ag(s)/AgCl(s)/Cl^-(aq, saturated KCl) reference electrode, a glassy carbon(GC) working electrode (3mm diameter), and a platinum wire counter electrode (0.2 mm diameter), fabricated in a 20 mL electrochemical cell. All experiments were performed with a computer controlled μ-Autolab modular electrochemical system (Eco Chemie U/techt, the Netherlands), driven with GPES software (Eco Chemie). Surface morphology was examined using Vega-Tescan electron microscope. A personal computer was used for data storage and processing.

2.3. Preparation of modified electrode

Firstly, the surface of the bare glassy carbon electrodes (GCE) was polished with 0.5 μm alumina (Al_2O_3) and then to remove alumina particles it was washed ultrasonically in ethanol for 3 miniutes. Following that, the GCE was immersed in a solution containing 1 mg/ ml DNA and the potential was repetitively cycled (20 scans) from -1.1 to 1.7 V at a scan rate of 100mV s^{-1} [33]. Further modification was performed by depositing MnO_x in situ on the DNA/GCE. Fig.1A displays continuous CVs (5 scans) for DNA/GC electrode in 1mM $MnSO_4.2H_2O$ solution containing 0.1 M Na_2SO_4 at the potential range of −0.8 to 1.8 V at 10 mVs^{-1}. The peak currents increased with continuous scanning, reflecting the continuous growth of manganese oxide nanospheres. These facts indicated that manganes oxide nanoparticles (MnO_xNps) were successfully deposited on the surface of DNA/GC electrode [41].

3. Results and discussion

3.1. Electrochemical and surface characterization of modified electrodes

The surfaces of MnOx /GCE and MnOxNsph/DNA/GCE were analyzed using SEM. The SEM images indicated that the MnOxNsphDNA/GCE is different in its size and shape from those of MnOxNPs /GCE. Fig.1B shows the morphology of MnOx/GCE which has nanostructured irregular-shape nanoseeds have been agglomerated and hav formed micron size. However, the SEM images of the MnOxNsph/DNA/GCE indicate the formation of nanosphere and regular-shape structures with average diameter of 80nm (Fig1C), when DNA templates are fixed on the suface of electrode.

(Fig.1)

The electrochemical impedance spectroscopy (EIS) is an effective and convenient tool to monitor the electrochemical behavior of the stepwise fabrication process of the modified electrode. Figure .2 shows impedance spectra represented as Nyquist plots (Zim vs. Zre) for bare GCE, DNA/GCE and MnOxNsph/DNA/GCE in 5 mM K3[Fe(CN)6]/K4[Fe(CN)6] as an electrochemical probe at 0.37 V and in the frequency range of $0.01–10^4$ Hz.

(Fig.2)

In EIS, the semicircle diameter equals the electron-transfer resistance (Rct), which controls the electron-transfer kinetics of redox probe at electrode interface. The electrochemical impedance spectroscopy data of the tested electrodes were fitted on a simple equal circuit, shown in Fig.2 (inset). In this circuit, Rs, C and Rct represent solution resistance, double layer capacitance and charge transfer resistance, respectively.

Curve (a) represents the EIS plot of bare GCE. After the assembly of DNA on electrode surface, the EIS of DNA/GC electrode generated more interfacial resistance (Curve b). This behavior can be related to electrostatic repulsion between negatively charged DNA/GCE surface and [Fe(CN)6]3-/4- probe. When MnOx as a nanosphere was assembled onto DNA/GC electrode, a dramatical decrease in the interfacial resistance was

observed (curve c). This proves that MnOx/DNA film enhances electron shuttling between reactant and the electrode surface.

3.2. Electrocatalytic oxidation of TU on MnO_xNsph/DNA /GCE

Cyclic voltammetry (CV) was used for the study of electro- oxidation of TU at the surface of different electrodes. Figure 3 shows the CV of modified and unmodified electrodes in the absence and presence of 3000 µM TU in a 0.1 M buffer solution of pH 7. At bare GCE (curve a), DNA/GCE (curve e) for GCE bare (curve c) and DNA/GCE (curve b) in the absence of TU and in the presence of TU no oxidation peak is observable. For MnO_xNsph/DNA in the presence of buffer (curve d), two oxidation peaks (OX1 and OX2) were observed for MnO_xNsph. In the presence of TU, oxidation peak currents (OX1 and OX2) dramatically increased, which may be due to electrocatalytic activity of MnO_xNsph (curve f).

Based on some previously published documents [42,46–51], a possible reaction mechanism between MnO_x and TU can be presented (equations 1 to 4):

$$Mn\ (III) \rightarrow Mn\ (IV) \qquad (1)$$

$$Mn\ (IV) + TU \rightarrow Mn\ (III) + [TU]_2^{2+} \qquad (2)$$

$$Mn\ (II) \rightarrow Mn\ (IV) \qquad (3)$$

$$Mn\ (IV) + TU \rightarrow Mn\ (III) + [TU]_2^{2+} \qquad (4)$$

As it is obvious, based on Fig 3d, peak OX1 can be attributed to the oxidation of Mn(III) to Mn(IV), while peak OX2 is related to the oxidation of Mn(II) to Mn(IV).

The anodic currents height of MnO_x increased in the presence of TU (Fig 3f). The enhancements of the oxidation peak currents were found to be linear over the studied concentration range.

Two anodic peaks for the oxidation of TU were observed. Two oxidation peaks can be related to disulfide formation by Mn (IV) for OX1 and OX2 [42].

The equations (1 and 2) and (3 and 4) show electrocatalytic mechanisms of TU for both OX1 and OX2 peaks by Mn (IV), respectivly.

(Fig.3)

In order to optimize the catalytic response of MnO_xNsph/DNA/GCE toward TU oxidation, the influence of pH solution on the response of MnO_xNsph/DNA/GCE to TU oxidation was investigated. Therefore, the CVs of the phosphate buffer solutions containing 500 µM TU at pH ranges 2 to 8 were recorded.

CVs are dependent on pH. In acidic media (pH 2-3), MnOx is unstable, indicating a large decrease in oxidation and reduction peaks [41]. Furthermore, DNA may be unstable in very acidic and basic media. Thus, the influence of pH solution on the response of MnO_xNsph/DNA/GCE to TU oxidation was investigated at natural pH values. It was previously reported that oxidation of TU just occurred at pH above 9. However, in this work, pH = 7 was selected as the optimal pH for subsequent uses.

The effect of the potential scan rate (for two oxidation peaks) on the response of the MnO_xNsph/DNA /GCE, immersed in phosphate buffer solution and containing 2000 µM TU (pH=7), was also investigated. The plots of oxidation and reduction peak currents (OX1 ,OX2 and Red) versus square root of scan rate are linear, indicating that the process is controlled by diffusion as expected for a catalytic system (Fig.4).

(Fig.4)

The performance of the proposed modified electrode (MnO_xNsph/DNA/GCE) in TU solutions with different concentrations was evaluated (Fig.5). It is obvious that this electrode has a rapid response and high sensitivity towards TU.

(Fig. 5)

For the anodic peaks (OX1 and OX2), the anodic peak currents of the waves, centered at 0.5 V and 0.95V, increased linearly with TU concentration. The plots of the peak currents versus TU concentrations (Fig. 5 (OX1 and OX2), Inset) reveals one linear range from 50 to 3000 µM for OX1 and 50 to 3000 µM for OX2 with a linear correlation (R^2 = 0.9846) and (R^2 = 0.9903) using cyclic voltammetric method, respectivly. The detection of limit

(signal to noise of 3), linear range and oxidation potential (Ep) were calculated for OX1, OX2 peaks (Table 1).

Since differential pulse voltammogram (DPV) is much more sensitive than cyclic voltammetry, it was employed to estimate the low detection limit.The differential pulse voltammogram of MnO_xNsph/DNA/GCE in the presence of different concentrations of TU, 4 to 3000 µM for OX1 peak and 4 to 2000 µM for OX2 peak, were recorded (Fig.6).

A linear dependence of catalytic currents *vs.* concentration of TU can be fitted in the equations I (µA) = 0.0069[TU] µAµM^{-1} +8.251 µA, and R^2 = 0.9846 for OX1 peak and I (µA) = 0.0381[TU] µAµM^{-1} + 17.364 µA, and R^2 = 0.9903 for OX2 peak. The detection limit (signal to noise of 3), linear range and Ep were calculated for OX1, OX2 peaks (Table 1).

(Fig. 6)

3.4. Interference effects

After the optimization and establishment of the determined method for the preparation of MnO_xNsph/DNA/GCE biosensor, the influence of various potential interfering compounds in real samples were studied on the determination of 200µ M TU.

The interferences of some anions such as NO_2^-, CN^-, NO_3^-, IO_3^-, SO_4^{2-}, I^-, Cl^-, Br^-, F^- and BrO_3^- on sensor were also examined with MnO_xNsph/DNA/GCE. According to the experimental results, these anions did not interfere in determining TU with 50 times TU concentration. The interference for NO_2^- appeared in equimolar concentration in their solution with TU. Other probable coexisting ions such as Na^+, K^+, Ca^{2+}, Mg^{2+}, Cu^{2+}, Zn^{2+},Al^{3+}, $Pb^{2+}$and Cd^{2+} ion did not interfere with determination either.

Various amino acids such as cysteine, methionine, glycine, phenylalanine, histidine, cystine and tryptophan were examined with respect to their interference with the determination of TU. Based on the experimental results methionine, glycine, cystine, phenylalanine and histidine did not interfere in determining TU with 50 fold excess over TU concentration. The interference for tryptophan and cysteine appeared in equimolar concentration in their solution with TU (Figs 7A and 7B were shown for methionine and cysteine, respectively).

(Fig. 7)

3.5. Repeatability and stability

TU concentration level of 500 µM was selected to examine the repeatability of voltammetric measurements of modified electrode (MnO_xNsph/DNA/GCE) in phosphate buffer (pH 7.0). The relative standard deviation (RSD) was found to be 5% for three successive assays. The long-time storage stability of the sensor was examined over a 26-day period. When the sensor was stored at room temprature and measured intermittently (every 2 days), the sensor retained about 86% of its original response after 2 days of storage. These results indicate good repeatability and stability for the proposed modified electrode for TU determination.

3.6. A comparison between the figures of merit of the proposed electrode and those of previous electrochemical sensors

The proposed electrode was compared with several other electrodes that have been developed for TU determination (The results are shown in Table 1). As it can be seen, the linear dynamic range, oxidation potentials (Ep), pH and lower detection limit of this work are comparable with or better than those of other works that are described in Table 1[43-46 and 52,53].

(Table. 1)

3.7. Analytical application

In order to demonstrate its practical application, this biosensor was used to determine TU in apple juice using the recommended procedure. 30 ml of apple juice was centrifuged at 500 rpm. Then, one milliliter was diluted to10ml of buffer sloution (pH7). The data which are given in Table 2 shows satisfactory results. Recoveries of 94.1-102.2 % of TU from juice sample (n = 4) were obtained using MnO_xNsph/DNA/GCE.

(Table. 2)

4. Conclusion

In the present work, we introduced a new modified electrode based on immobilizing of MnO_xNsph/DNA on glassy carbon electrode. The electrodeposition method was used for the synthesis of MnO_xNsph onto the bare GCE and DNA/GCE surfaces. The SEM measurements revealed the formation of MnO_xNsph deposited on the DNA/GCE surface, while the electrodeposition of MnO_xNsph on the bare GCE surface leads to the formation of irregular-shape nanoseeds agglomerated micron size. The MnO_xNsph/DNA/GCE showed very efficient catalytic activity in the electrochemical oxidation of TU.The best voltammetric peak current was obtained at natural pH. As compared in Table 1, the proposed electrode has advantages in detection limit Ep, pH and linear range with respect to more reported works in this Table. This method of assembling MnO_xNsph on the DNA template may be expanded to other nanoparticles and is expected to have promising implication in the design of electrochemical biosensors or sensors.

Acknowledgments

This reasearch was financially supported by Vice-Chancellor in Research Affairs of Kurdistan University of Medical Sciences, and registerated by **IR.MUK.REC.1395/234** serial number. The authors gratefully acknowledge the support of the Environmental Health Research Center, Kurdistan University of Medical Sciences, for laboratory support, and material preparation.

Legends to the Figures:

Fig.1 (A): The continuous CVs for the DNA/GCE electrode in 1mM $MnSO_4.2H_2O$ solution containing 0.1 M Na_2SO_4 at 10 mVs^{-1}. **(B)**: SEM image of MnO_x /GCE (C).SEM image of MnO_xNsph/DNA/GCE

Fig.2. Electrochemical impedance spectroscopy (EIS) of (a) bare GC electrode; (b) DNA/GC electrode; (c) MnO_xNsph/GC electrode in 5mM probe $Fe(CN)_6^{4-/3-}$ (Inset). Fitted circuit for the electrochemical impedance spectroscopic data DNA/GCE and MnO_xNsph/DNA/GCE

Fig.3. Cyclic voltammetry response of a bare GCE (curves a and c) in the absence of TU and in the presence of TU, DNA/GCE (curves b and e) in the presence and absence of TU. MnOxNsph/DNA/GCE (curves d and f) in the absence and presence of TU

Fig.4. (a) Cyclic voltammetry response of a GCE modified with MnO_x/DNA nanocomposite in a phosphate buffer (pH 7) containing 2000µM of TU at scan rates of (inner to outer) 10, 20, 30, 40, 50, 60, 70, 80, 90, 100mVs^{-1} ,and plots of peak current vs. scan rate and square root of scan rate for OX1 and OX2 peaks

Fig.5. Cyclic voltammograms of MnO_xNsph/DNA modified GCE in buffer solution pH 7 with increasing TU concentrations; plots of peak current vs. TU concentrations for OX1 and OX2 peaks

Fig.6. DPV of MnO_xNsph/DNA/GCE modified GC electrode in pH =7 buffer containing different concentration of TU. Inset plots of peak current vs TU concentrations for OX1 and OX2 peaks.

Fig.7. Cyclic voltammograms of MnO_xNsph/DNA/GCE modified electrode in pH=7 buffer containing (A) (a) TU, (b) TU and methionine (B) (a) TU, (b) TU and cysteine.

Table.1. Analytical parameters of several modified electrodes for determination of TU

Table.2. Determination of TU in a real sample

References

[1] F. D. Snell, Photometric and Fluorimetric Methods of Analysis, Parts I and II. Wiley, New York, 1978.

[2] S. Hirzel, Thioharnstoff, BUA-Stoffbericht 179, Stuttgart, 1995.

[3] S.Sohan, A.G.Bindra, S.S.Cheema,W.S.Dhillon, J of Plant Science Reasearch.7 (1991) 40-41.

[4] Z. He, F. Wu, H. Meng, L. Ling, L. Yuan, Q. Luo, Y. E. Zeng, Anal. Sci 15(1999)381-84.

[5] K. R. Koch, Coord. Chem. Rev.216-217 (2001) 473-488.

[6] P. Calza, C. Medana, C. Baiocchi, E. Pelizzetti, Journal of Photochemistry and Photobiology A: Chemistry. 189 (2007) 380 -86.

[7] M. H. Chao, B. M. Kariuki, K. D. M. Harris, S. P. Collins, D. Laundy,Angew. Chem. Int. Ed. 42(2003) 2982-85.

[8] H. S. S. Ramakrishna Matte, A. Gomathi, A. K. Manna, J. D. Late, R. Datta, C. N. R. Rao, Angew. Chem. Int. Ed. 49 (2010) 4059 –4062.

[9] A. Modi , K. Shukla , J. Pandya , K. Parmar, International Journal of Emerging Technology and Advanced Engineering,2 (2012) 599-606.

[10] World Health Organization (WHO). Thiourea.Geneva, 2003.

[11] M.M. Milosavljevici, I.M. Vukicevic, S. D. J. Nikliic, A. Marnkovic, S. Krstic, S. Petrovic, J. Serb. Chem. Soc 81 (3) (2016) 219–231.

[12] J. Rethmeier, G. Nemann, C. Stumpf, A. Rabenstein, C. Vogt, J. Chromatogr A 934(2001)129-34.

[13] J. Kurzawa, K. Janowicz, Anal Bioanal Chem 382 (2005) 1584-89.

[14] A Raffaelli, S. Pucci, R. Lazzaroni, P. Salvadori, Rapid Commun Mass Spectrom 11(1997)259-64.

[15] K.Kargosha, M. Khanmohammadi, M. Ghadiri, Anal Chim Acta 437(2001)139-43.

[16] H.J. Bowley, E.A. Crathorne, D.L. Gerrard, Analyst 111(1986)539-42.

[17] A.L. Fornazari, W. T. Suarez, J. Vieira, F. O. Fatibello, Acta Chim. Slov 52 (2005) 164-167.

[18] D. L. Rabenstein, G. T. Yamashita, Anal. Biochem 180 (1989) 259-263.

[19] J. L. D. Eramo, A. E. Finkelstein, F.Q. Boccazzi, O. Fridman, J. Chromatogr B: Biomed. Sci. Appl 720 (1998) 205-263.

[20] P. J. Vandeberg, D. C. Johnson, Anal. Chem 65 (1993) 2713-8.

[21] M. A. Riquelme , M. A. Lucero, M. Villagrán, M. C. Arévalo, H. J. Hernández-Creus , M. Velez , J. Aguirre, R. Arce, G. Ramírez. Int. J. Electrochem. Sci 7 (2012) 9738-47.

[22] V. Mani, A. T. Vilian, E. S. Chen, Int. J. Electrochem. Sci, 7 (2012) 12774-85.

[23] O. F. Filho, E. R. Dockal, L. H. M. Junior , M. F. S. Teixeir. Analytical Letters, 40 (2007) 1825-1852.

[24] N. F. Atta, A. Galal, S. M. Azab. Electroanalysis 24 (2012) 1431- 40.

[25] N. T. Rosie, T. Chelfi, B. Hach, H. B. B. Massai, Laura1, N. Chtaini, Bulletin of the Catalysis Society of India 9 (2010) 68-73.

[26] C. Yunchun, L. Zhousheng, Y. Xianwen, Materials and Design 28 (2007) 722–725.

[27] S.R. Ede,A.Ramadoss,S. Anantharaj, U. Nithiyanantham, S.Kundu, Phys. Chem. Chem. Phys, 16 (2014)21846-21859.

[28] J.R.Lakwicz, I.Gryczynski, Z.Gryczynski, K.Nowaczyk, C.J.Murphy, Anal. Biochem. 280(2000)128–136.

[29] T. Scheibel, R. Parthasarathy, G. Sawicki, X. M. Lin, H. Jaeger, S. L. Lindquist, Natl. Acad. Sci. U. S. A 100 (2003) 4527-32.

[30] S. W. Lee, C. B. Mao, C. E. Flynn, A. M. Belcher, Science 296 (2002) 892-95.

[31] M. R. Jones, R. J. Macfarlane, B. Lee, J. Zhang, K. L. Young, A. J. Senesi, C. A. Mirkin, Mater 9 (2010) 913-17.

[32] A. V. Pinheiro, D. R. Han, W. M. Shih and H. Yan, Nat.Nanotechnol, 6 (2011) 763-72.

[33] E.Sharifi, A. Salimi, E. Shams, A. Noorbakhsh,M.K. Amini, Biosens Bioelectron, 56 (2014) 313–319.

[34] M. Zheng, A. Jagota, E. D. Semke, B. A. Diner, R. S. McLean, S. R. Lustig, R. E. Richardson,N. G. Tassi, Nat. Mater 2 (2003) 33842.

[35] S. Kudu, M.M. Jayachandran, RSC Adv 3(2013)16489-98.

[36] D. Majumdar, A. Singha, P. K. Mondal, S. Kundu, ACS Appl. Mater. Interfaces, 5 (2013) 7798-7807.

[37] S. Kundu, K. Wang, D. Huitink, H. Liang, Langmuir 25(2009) 10146-52.

[38] C. F. Monson, A. T. Woolley, Nano Lett 3 (2003) 359-63.

[39] D. Sarker, M. Mandal, J. Phys. Chem. C 116 (2012) 3227-34.

[40] S. Kundu, H. Lee, H. Liang, Inorg. Chem 48 (2009) 121-7.

[41] S. M. Majda, H. Teymourian, , Electrochimica Acta 108 (2013) 707-716.

[42] M. Iwamoto, R.A. Osteryoung, J. Electroanal. Chem. Interfacial Electrochem 169 (1984) 181–194.

[43] F. Manea, C. Radovan, J. Schoonman, J. Appl. Electrochem 36(2006) 1075–1081.

[44] A. Levent, E. Keskin, Y. Yardım, Z. S¸ entürk, Rev.Anal. Chem,30 (2011) 45-51.

[45] D. Nematollahi, M.Rafiee, Sensors, 3 (2003) 534–543.

[46] I. Corb, F. Manea, C. Radovan, A. Pop, G. Burtica, P. Malchev, S. Picken, J. Schoonman ,Sensors, 77(2007)2626–2635.

[47] M.R. Mahmoudian, Y. Aliasa, W.J. Basirun, Pei Meng Woi, M. Sookhaki

Sensors and Actuators B 201 (2014) 526–534.

[48] K. Ding ,Journal of the Chinese Chemical Society,56(2009) 175-181

[49] S. Mansouri Majda, H. Teymouriana, R. Hallaj, Electrochimica Acta 108 (2013) 707– 716.

[50] M.Tu, H.Chen, Y. Wang, M. Moochhal, P. Alagappan, B. Liedberg , Analytica Chimica Acta, 853 (2015) 228–233.

[51] N. Spataru, T. Spataru, A. Fujishima, Electroanalysis 17(2005)800–805.

[52] A. Safavi, R. Ahmadi, F.A. Mahyari, M Tohidi, Sensors and Actuators B: Chemical 207 (2015) 668-672.

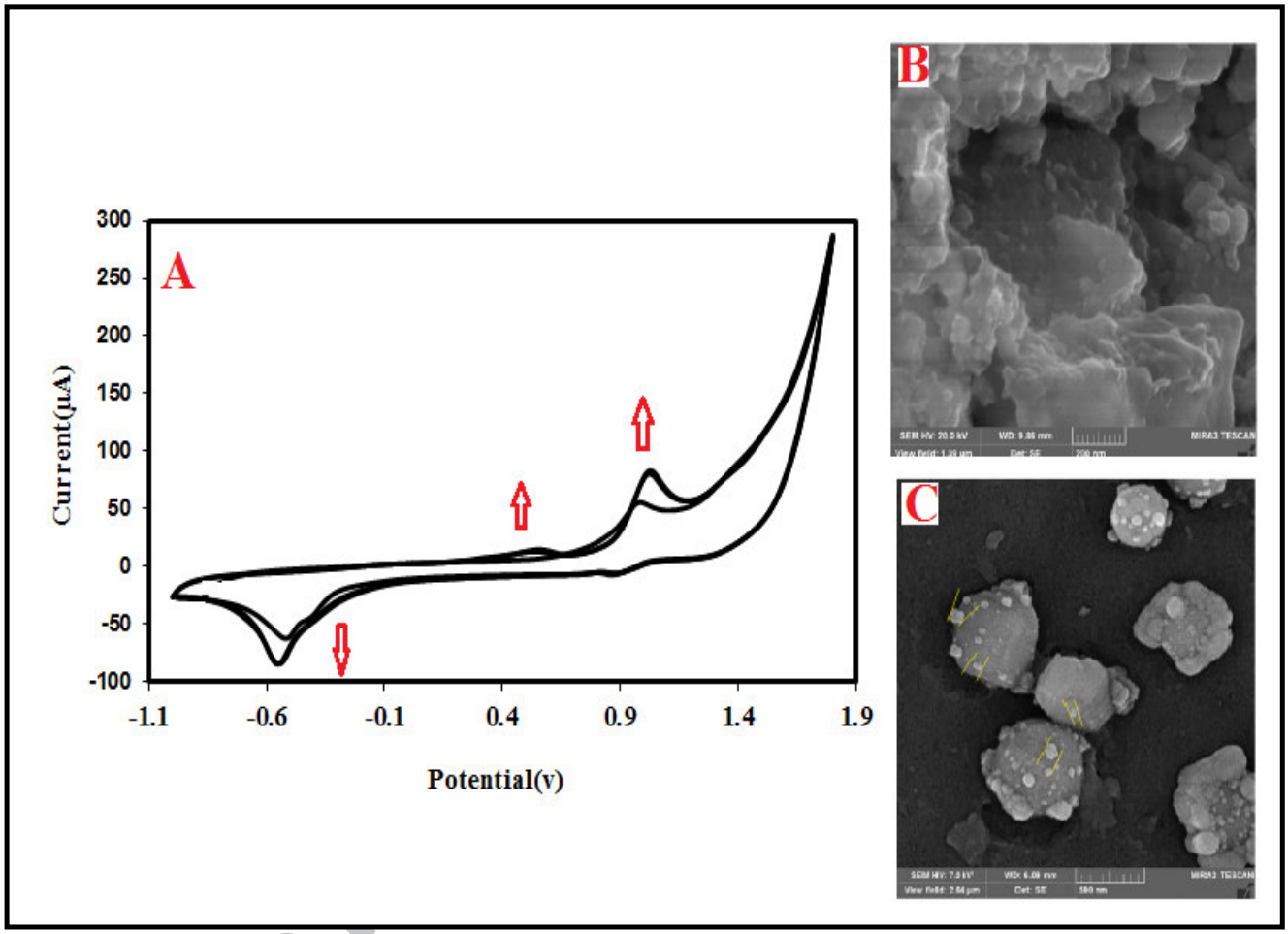
A
B
C
Current(μA)
Potential(v)
300
250
200
150
100
50
0
-50
-100
-1.1
-0.6
-0.1
0.4
0.9
1.4
1.9

Fig.1

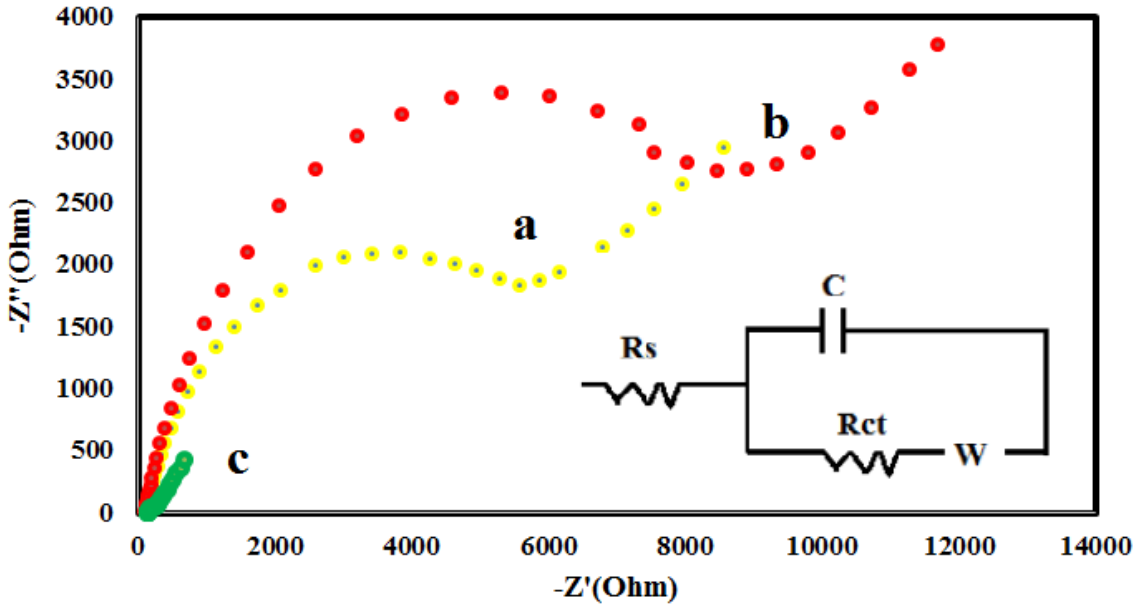

Fig.2

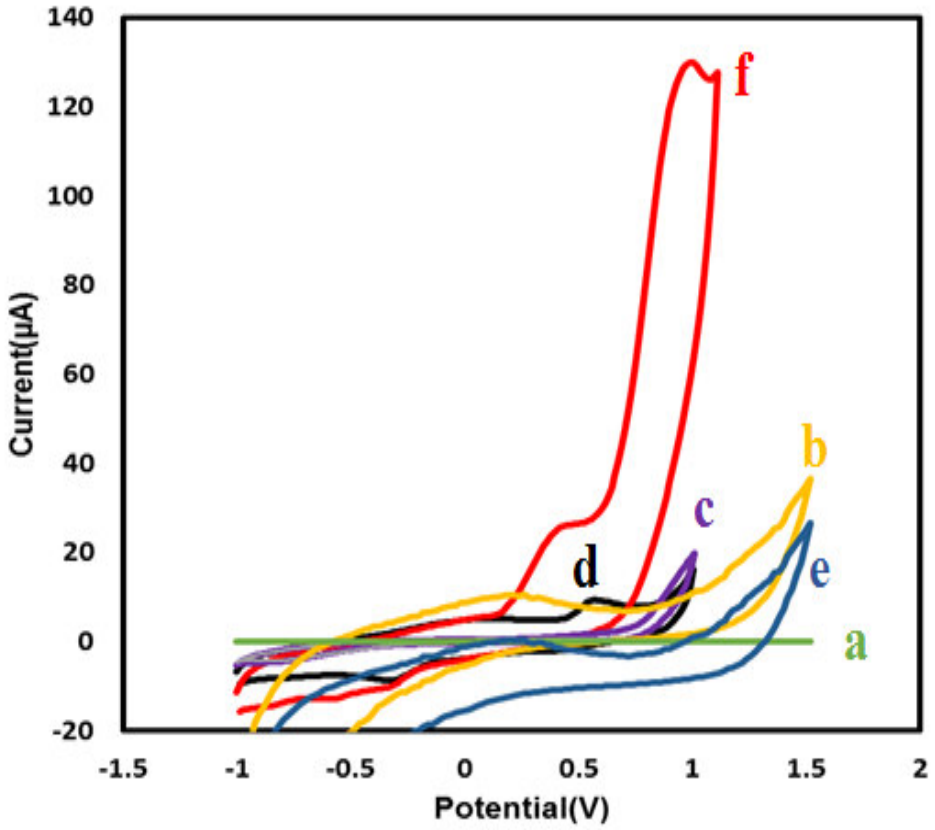

Fig.3

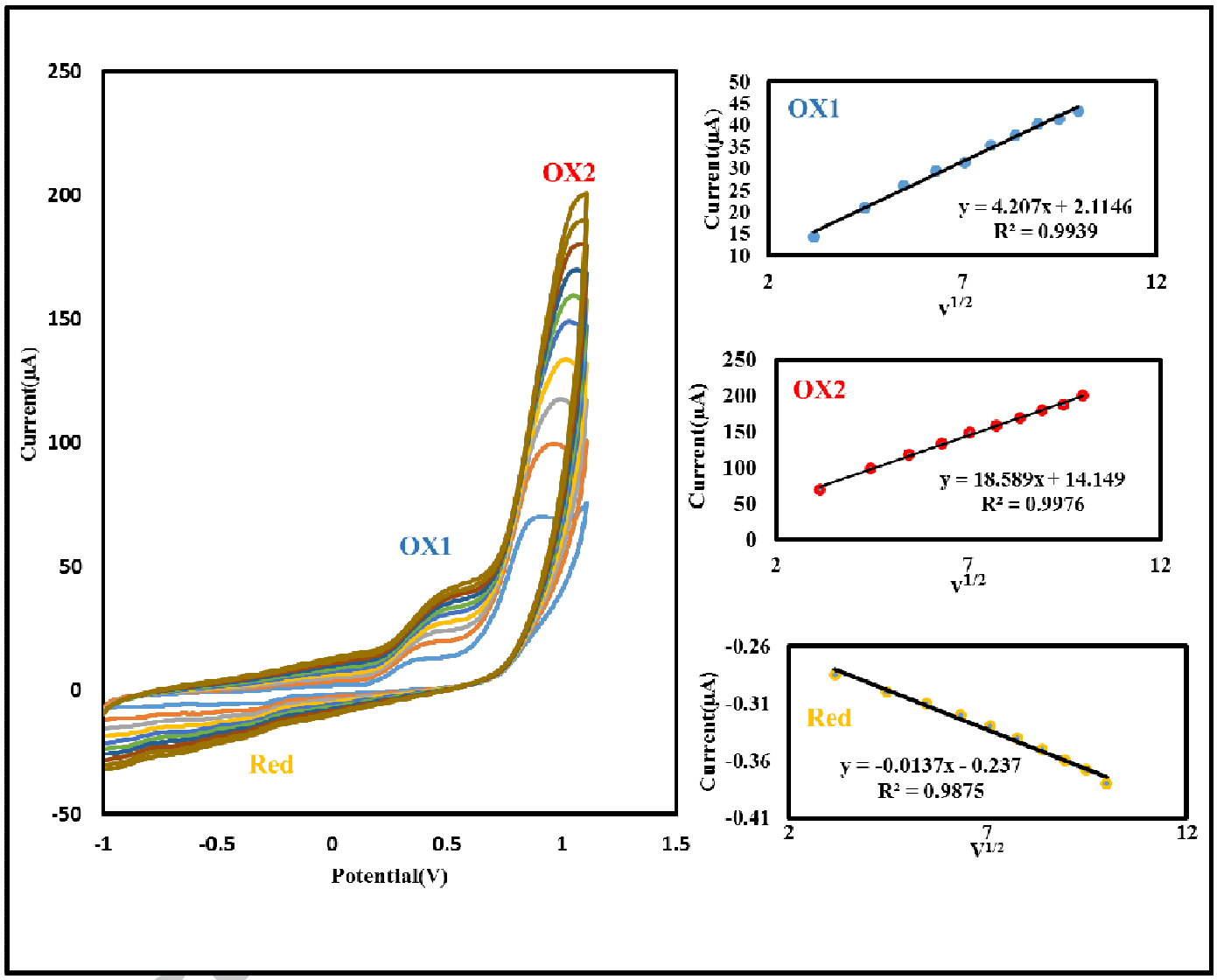
OX2
OX1
Red
Current(μA)
Potential(V)
OX1
y = 4.207x + 2.1146
R² = 0.9939
OX2
y = 18.589x + 14.149
R² = 0.9976
Red
y = -0.0137x - 0.237
R² = 0.9875
v^1/2

Fig.4

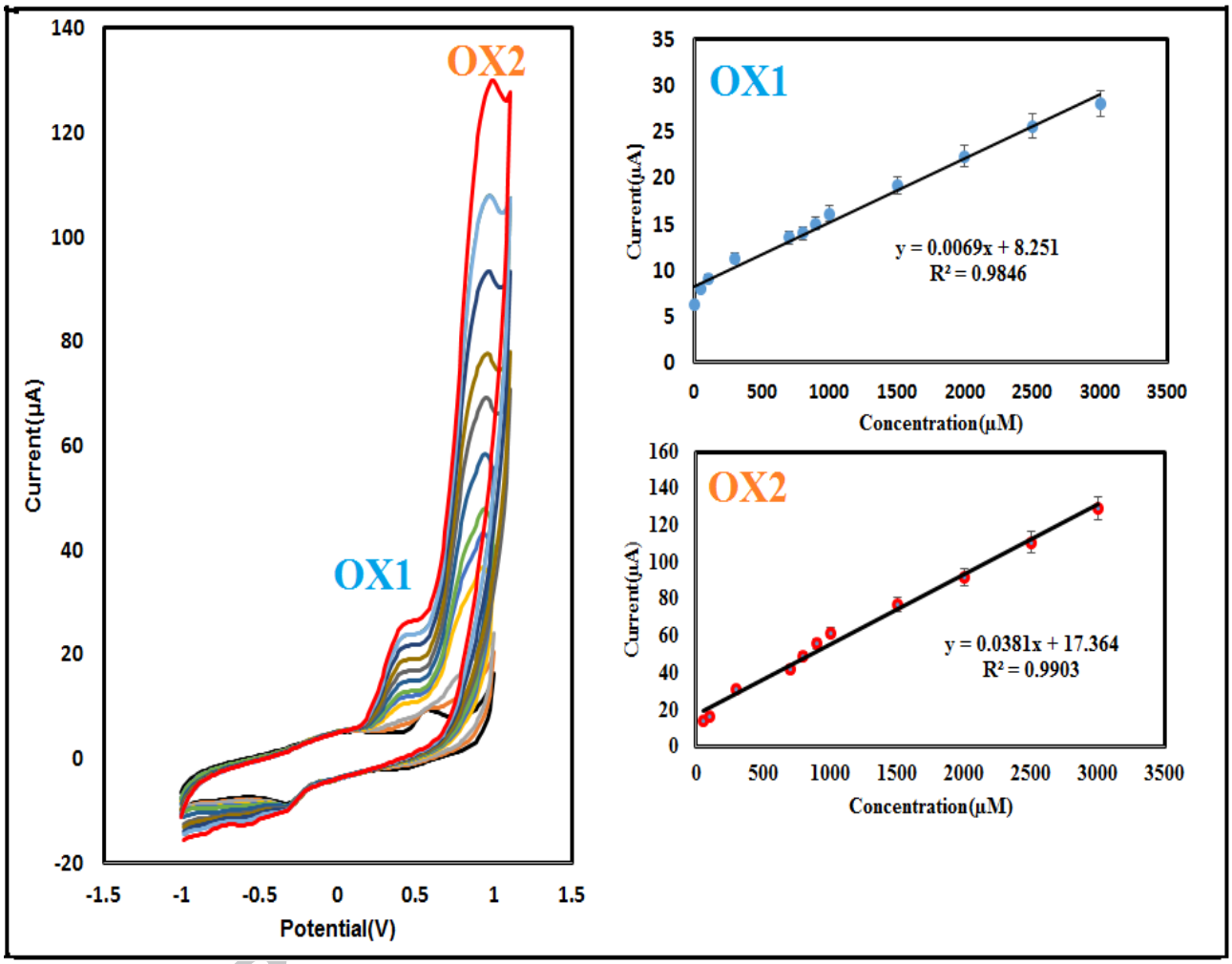
OX2
OX1
Current(µA)
Potential(V)
140
120
100
80
60
40
20
0
-20
-1.5
-1
-0.5
0
0.5
1
1.5
OX1
y = 0.0069x + 8.251
R² = 0.9846
Current(µA)
Concentration(µM)
35
30
25
20
15
10
5
0
0
500
1000
1500
2000
2500
3000
3500
OX2
y = 0.0381x + 17.364
R² = 0.9903
Current(µA)
Concentration(µM)
160
140
120
100
80
60
40
20
0

Fig.5

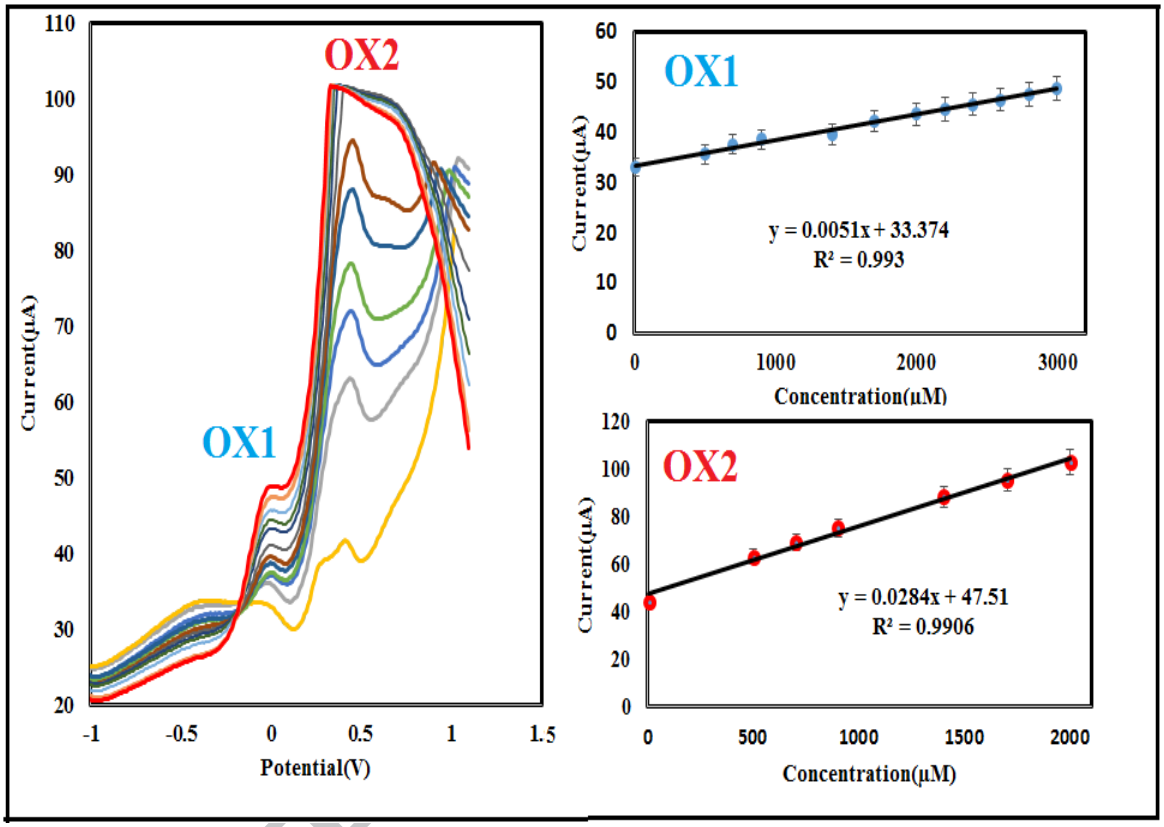

Fig.6

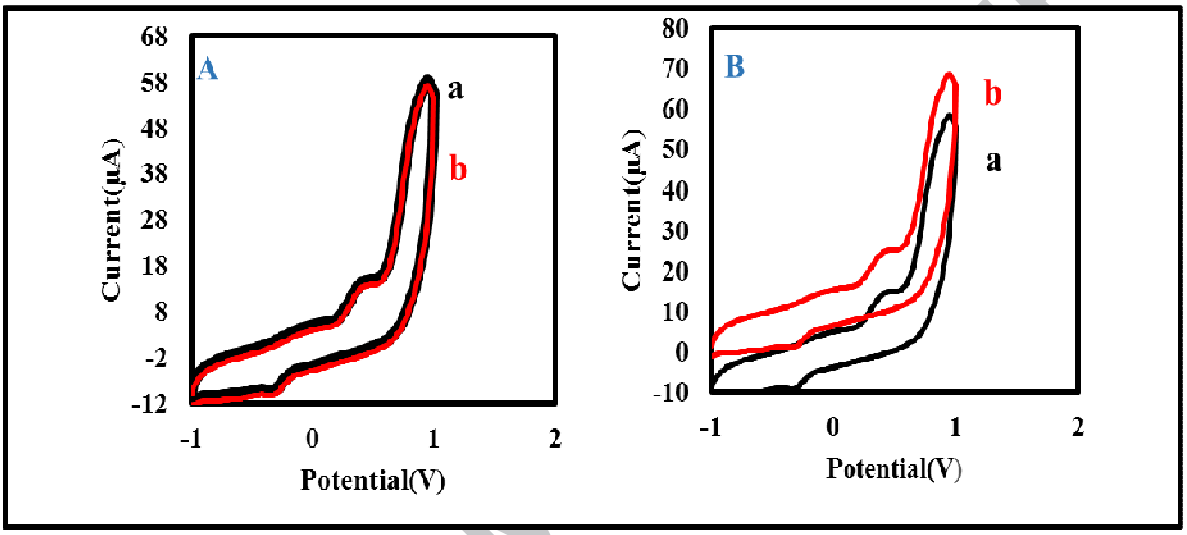

Fig.7

Table. 1 Analytical parameters of several modified electrodes for determination of TU

Electrode	pH	Ep	LOD (µM)	Linear range	Ref.
Boron-doped diamond	1.8	1.1	9.37	4-8000	51
Copper oxide–Copper	NaOH	0.625	_	1000-8000	43
Pencil graphite electrode	12	0.95	1.29	6.3-30	44
Alumina modified Pt	4.5	0.345	4.8	25-7000	45
Carbon-based composite electrode	-	- -	20	100-1000 500-4000	46
graphene nanosheets–Ag nanoparticles hybrid ionic liquid electrode.	NaOH	-0.2	0.7	1-3000	52
This work(CV-OX1)	7	0.39	14	50-3000	-
This work(CV-OX2)	7	0.95	22	50-3000	-
This work(Diff-OX1)	7	0	7	4-3000	-
This work(Diff-OX2)	7	0.45	1	4-2000	-

Table.2. Determination of TU in a real sample

Sample	Added(μM)	Found(μM)	Recovery(%)
1	-	Not detect	-
2	10	9.41	94.1
3	200	201.1	100.5
4	300	306.6	102.2